

What happens when cardiac Na channels lose their function? 1 – Numerical studies of the vulnerable period in tissue expressing mutant channels

C. Frank Starmer^{a,*}, Thomas J. Colatsky^b, Augustus O. Grant^c

^aDepartments of Biometry/Epidemiology and Medicine (Cardiology), Medical University of South Carolina, Suite 200 I Administration/Library, 171 Ashley Ave, Charleston, SC 29425, USA

^bDepartment of Pharmacology, Medical University of South Carolina, Charleston, SC 29425, USA

^cDepartment of Medicine (Cardiology), Duke University Medical Center, Durham, NC 27706, USA

Received 9 April 2002; accepted 19 July 2002

Abstract

Objective: The vulnerable period (VP) defines an interval during which premature impulses can trigger reentrant arrhythmias leading to ventricular fibrillation and sudden death. The mechanistic basis of the success or failure of impulse propagation during the VP remains unclear. Recent clinical reports of gene mutations, drugs and cardiac disease link a variety of often lethal conditions with loss of cardiac Na channel function (NaLOF) and reentrant proarrhythmia. We hypothesized that during the VP, the Na conductance at the stimulus site is graded and that NaLOF would favor reentry specifically by flattening this gradient, which would destabilize antegrade front formation. **Methods:** Using numerical studies of propagation in a one-dimensional cable of ventricular cells, we identified the boundaries of the VP using paired (s1–s2) stimulation. We explored VP alterations associated with different NaLOF scenarios including reduced channel density, accelerated rate of inactivation, and prolonged recovery from inactivation. **Results:** Following the passage of a wave over the s2 site, a gradient in the restoration of Na channel conductance was demonstrated to exist during the VP. The VP boundaries coincided with different thresholds for stable retrograde and antegrade impulse propagation. Reducing channel density, accelerating inactivation and slowing the recovery from inactivation flattened the restoration gradient and extended the VP. VP extension was directly proportional to the time constant of Na channel recovery. **Conclusions:** Mutations that accelerate inactivation, slow recovery from inactivation, or reduce Na channel density flatten the restoration gradient within the VP which prolongs the VP and increases the probability that a premature impulse will initiate reentry. These studies define a new mechanism that links alterations in Na channel function with conditions that enable premature excitation to generate proarrhythmia and sudden death.

© 2002 European Society of Cardiology. Published by Elsevier Science B.V. All rights reserved.

Keywords: Arrhythmia (mechanisms); Computer modelling; Conduction (block); Impulse formation; Na-channel; Ventricular arrhythmias

1. Introduction

The initiation of reentry requires that a premature impulse arises within a vulnerable region where propagation succeeds in some directions and fails in other directions. The vulnerable period (VP) reflects the transit of this region across the site of premature excitation, but the

sequence of events underlying the development of a successfully propagating reentrant wave is uncertain. Mines [1] and later Wiggers and Wegria [2] demonstrated that single stimuli could initiate reentry and fibrillation if timed to occur within a VP trailing an earlier wave of activation. Wiener and Rosenbleuth (W–R) [3] viewed the VP as the transit of the refractory boundary across the suprathreshold length, L , of a stimulating field and thus established a mechanistic basis for the VP. With s1–s2 stimulation, Allesie and coworkers [4] confirmed the

*Corresponding author. Tel.: +1-843-792-0215; fax: +1-843-792-0258.

E-mail addresses: <http://people.musc.edu/~starmef> (C.F. Starmer), starmef@musc.edu (C.F. Starmer).

Time for primary review 30 days.

existence of a bounded VP consistent with the W–R paradigm. Numerical studies of reentry in a two-dimensional sheet by VanCapelle and Durrer [5] supported the W–R model, provided numerical estimates of the VP and showed how front formation within the vulnerable region led to spiral wave reentry. Later, Joyner [6] identified spatial asymmetry in some membrane property as an essential requirement for producing unidirectional block in a one-dimensional cable. Quan and Rudy [7] extended these studies by incorporating gap junction connections between cells in their cable model. Using paired s_1 – s_2 stimulation to create the asymmetric excitability, they explored unidirectional block as a function of s_1 – s_2 delay and demonstrated that cellular uncoupling both slowed propagation and extended the VP, confirming the W–R model in a non-uniform cable.

Understanding vulnerability is critically dependent on characterizing the ability of a propagating front to recruit a sufficient amount of Na current to maintain propagation. Cardiac sodium channel mutations [8,9], myocardial ischemia [10] and use-dependent sodium channel blockade [11] are known to alter the amount of Na current available for propagation either by reducing Na channel density or by changing the dynamics of channel state transitions, and all are associated with enhanced proarrhythmia. Assuming that Na current is adequate to support propagation, then in resting normal myocardium, excitation of a cluster of cells will form a front that will propagate in all directions away from the site of activation. However, the response to re-excitation after passage of an excitatory front will vary depending on the local value of the effective Na conductance and its spatial distribution.

Trailing an action potential is a region of recovery from Na channel inactivation. This restoration gradient of Na conductance provides a spatial asymmetry in excitability and the potential for a unidirectional response to stimulation. The existence of the VP suggests that the Na conductance restoration gradient in a region of marginally excitable cells might be critical during formation of stably propagating antegrade and retrograde waves, and thus provide a mechanistic link between loss of Na channel function (NaLOF) and proarrhythmia.

We previously showed that drug-induced blockade of cardiac Na channels altered the VP, and demonstrated an association between use-dependent blockade and extension of the VP using both numerical [12,13] and *in vitro* approaches [14,15]. These studies indicated that the VP could be prolonged beyond that predicted by theoretical models [3,13], and that NaLOF secondary to use-dependent Na channel blockade had both antiarrhythmic and proarrhythmic properties. Our analysis indicated that slowed restoration of Na channel conductance not only extended the refractory period, an antiarrhythmic process, but also extended the VP, a proarrhythmic process, thereby increasing the probability of triggering reentry with an unsuppressed premature ventricular contraction (PVC).

Arrhythmogenic mutants of SCN5A [8,9] and cells isolated from ischemic border zones [10] display NaLOF similar to the effects of Class I antiarrhythmic drugs. The alterations in mutant channel gating properties should have relatively small effects on steady-state uniform propagation. However, their effect on propagation under non-steady-state conditions, e.g. following re-excitation within the VP, is unknown and could significantly alter the dynamics of front formation or collapse thereby amplifying the VP.

In the present study, we use numerical studies to explore the VP in a one-dimensional cable under normal conditions and in the presence of a variety of Na channel gating changes associated with known Na channel mutations, including slowed recovery from Na channel inactivation and accelerated inactivation. We observed a gradient of Na conductance within the VP and different thresholds of Na channel conductance at the most and least premature boundaries of the VP, one representing the minimum conductance required to establish stable retrograde propagation and a larger one representing the minimum conductance required to establish stable antegrade propagation. Accelerating inactivation, slowing the recovery from inactivation and reducing the density of Na channels flattened the Na conductance restoration gradient within the VP and extended the VP. In the companion paper [16], we expand this observation by exploring the relation between VP extension and voltage-dependent Na channel blockade.

2. Methods

We explored the boundaries of the vulnerable period in a one-dimensional cable of cardiac cells. To reduce confounding influences of multiple currents we used the Beeler-Reuter (BR) [17] ventricular model replacing the BR Na channel model with the Ebihara–Johnson model [18] and using a maximal Na conductance, G_{Na} , of 24.25 mS/cm² for normal conditions. A 5-cm cable was constructed by linking excitable segments having an axial resistivity of 250 ohm cm and a cell radius of 7 μ m. The cable was discretized with space steps of 1/512 cm and time steps of 1/128 ms. The discretized equations were solved using an implicit method. The boundary conditions at the ends of the cable permitted no current flow ($\partial V/\partial x = 0$). We defined the spatially distributed effective Na conductance, $g_{Na}(x)$, in terms of the maximum conductance, G_{Na} and the degree of channel inactivation as

$$g_{Na}(x) = G_{Na}h(x)j(x) \quad (1)$$

where $h(x)$ and $j(x)$ are the spatial distributions of fast (h) and slow (j) non-inactivated channels.

We defined the VP in a cable as the range of s_1 – s_2 delays resulting in unidirectional propagation. We measured the VP by initiating a conditioning wave (s_1) at one

end of the cable, and after a suitable delay (s1–s2) initiating a test wave (s2) with a stimulus introduced at 1.25 cm from one end (Fig. 1). The stimulus amplitude and duration of both conditioning (s1) and test (s2) stimuli were $-62.5 \mu\text{A}/\text{cm}^2$ and 0.25 ms, respectively, and the length of the s2 electrode was 1/512 cm. While varying the s1–s2 delay we identified the most premature boundary marking the transition from a refractory response (collapsing wave) to stable retrograde propagation and the least premature boundary marking the transition from a collapsing antegrade front to stable antegrade propagation. The effects of reduced Na channel density were explored by varying G_{Na} from $24.25 \text{ mS}/\text{cm}^2$ (control or wild type) to $6.0 \text{ mS}/\text{cm}^2$, a value near the threshold for stable propagation. The effects of slowed recovery from Na channel

inactivation were explored by reducing the recovery rate constant, α_j , by 3, 5 and 10. Accelerated inactivation was explored by doubling the inactivation rate, β_n .

3. Results

We explored front formation in the presence of a gradient in effective Na conductance, $g_{\text{Na}}(x)$, using s1–s2 pairs to locate the antegrade (least premature) and retrograde (most premature) VP boundaries. Fig. 1 displays the membrane potential profiles for s1–s2 delays bounding the VP and plotted at 5-ms intervals in order to visualize the temporal progression of front development. Depicted here are two conditions: normal cells (panels A–D; $G_{\text{Na}} =$

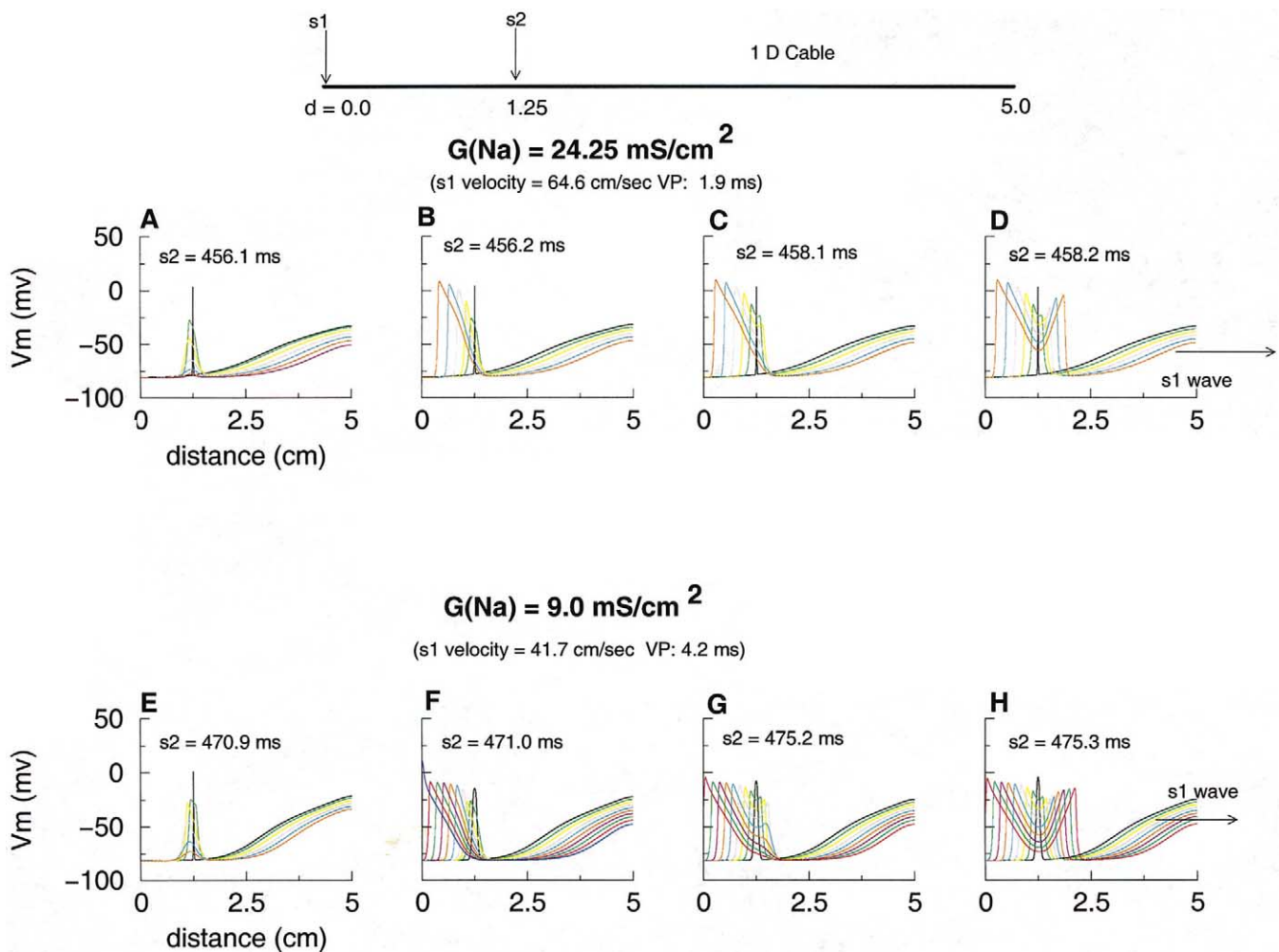


Fig. 1. Identification of the vulnerable period with paired s1–s2 stimuli. Each test consisted of a conditioning wave (s1) initiated by injecting current into the left end of a 5-cm excitable cable, followed by test stimuli (s2) injected at 1.25 cm. The responses to variations in s1–s2 delay were noted and the membrane potential at 5-ms intervals was plotted at the transition from refractory (A,E) to stable retrograde propagation (B,F) and from retrograde (C,G) to stable antegrade propagation (E,H). Panels A–D represent the responses to s2 stimulation with a normal Na conductance ($G_{\text{Na}} = 24.25 \text{ mS}/\text{cm}^2$), while panels E–H represent the responses to s2 stimulation in a cable of cells with a reduced sodium conductance similar to that observed in ischemic border zone cells [3] ($G_{\text{Na}} = 9.0 \text{ mS}/\text{cm}^2$). While the s1 velocity decreased from 64.6 to 41.7 cm/s (ratio of 1.55), the VP increased from 1.9 to 4.2 ms (ratio of 2.2). The dynamics of forming a stably propagating antegrade wave was sensitive to G_{Na} . At the transition to stable antegrade propagation there was a brief interval of decremental antegrade propagation followed by incremental conduction and subsequent evolution of stable antegrade propagation. Reducing G_{Na} increased the duration of the interval of decremental antegrade propagation as seen in panels C and G.

24.25 mS/cm²) and cells with reduced Na conductance (panels E–H; $G_{Na}=9.0$ mS/cm²). This reduced level of G_{Na} is consistent with the changes seen in ischemic border zone cells [10] (panels E–H). Panels A, B and E, F display the transition from refractory (collapsing impulse) to stable retrograde propagation at the most premature boundary of the VP. Panels C, D and G, H display responses at the least premature boundary of the VP, reflecting the transition from collapse of the antegrade front to stable antegrade propagation. The VP increased more than 2-fold from 1.9 to 4.2 ms while the velocity changed by less than a factor of 2, in conflict with results expected from transit of the refractory boundary across the stimulus field [3,13]. In addition, the temporal progressions of antegrade front collapse (panels C and G) were quite different, with the antegrade front collapsing almost immediately when $G_{Na}=24.25$ mS/cm² but requiring ~ 35 ms of decremental propagation before collapse when $G_{Na}=9.0$ mS/cm².

Propagation succeeds when the leading edge of the action potential can open enough Na channels from adjoining regions (a recruiting process) to supply the current required to extend the recruiting process and maintain stable propagation. We visualized the ‘capture’ range of a propagating front as determined by the space constant. We reasoned that propagation should succeed as long as the density of available channels per space constant was adequate to meet the ignition requirements for advancing the front.

We defined the recruiting capacity as a function of the spatial gradient of recovering Na channels (the restoration gradient) and the space constant. Exploring the role of the restoration gradient on wave front development, we plotted the spatial distribution of the effective Na channel conductance ($g_{Na}(x) = G_{Na} h(x) j(x)$) at the s1–s2 delays associated with the most premature boundary of unidirectional conduction and at the s1–s2 delay associated with the least premature boundary of unidirectional conduction for G_{Na} ranging from 24.25 to 6 mS/cm² (Fig. 2). The conductance profiles for each value of G_{Na} intersected within very small regions, representing thresholds of stable retrograde (5.02 mS/cm²) and stable antegrade (5.25 mS/cm²) propagation. The threshold for stable retrograde propagation was slightly greater than that determined in a resting cable with no Na conductance restoration gradient ($g_{Na}=4.87$ mS/cm²).

Injecting current greater than threshold into the s2 electrode produced a localized region of depolarizing potential. The potential nearest the center of the electrode was suprathreshold while the potential outside this region was subthreshold. We defined the suprathreshold region as the stimulus field. With no gradient, excitation opened channels symmetrically within the stimulus field. With a gradient of conductance, excitation opened (recruited) fewer channels in the antegrade direction than in the retrograde direction. In order to compensate for the lower

density of antegrade channels, the threshold for stable retrograde propagation, T_r , was larger than the minimum required for a resting cable. Establishing a stably propagating antegrade wave required exceeding a threshold, T_a , that was larger than T_r because the antegrade front had to propagate into less recovered medium as shown in Fig. 2. The result was extension of the VP beyond that associated with the transit of T_r across the suprathreshold region of the s2 field, by an additional distance determined by the restoration gradient (Fig. 2A). Table 1 summarizes the measurements of the refractory period, RP, vulnerable period, VP, the s1 velocity and the effective conductance gradient at the thresholds for stable retrograde and antegrade propagation.

We plotted (Fig. 3) the refractory period, RP (panel A), VP (panel B) and the probability of unidirectional propagation, p(UP) (panel C) in order to assess the relationship between antiarrhythmic and proarrhythmic potential. We estimated the probability as the ratio of the VP to the excitable interval: $p(UP) = VP/(RR - RP)$ where RR is the R–R interval. We assumed a heart rate of 75 (800-ms interval). At high values of G_{Na} there were only small changes in the VP relative to the RP while at low values of G_{Na} , a 10% increase in RP (from 456.7 to 500.7 ms) led to a 5-fold increase in the VP (from 1.9 to 11.2 ms) and a 7-fold increase in p(UP) from 0.005 to 0.037.

Some Na channel mutations associated with arrhythmogenic processes exhibited slowed recovery from channel inactivation. We approximated this situation by reducing the rate constant for recovery from inactivation, α_r , by a factor of 3. This shifted the inactivation curve 4.5 mV in the hyperpolarizing direction similar to that observed in Ref. [10] (Fig. 4A) and increased the time constant of recovery by a factor of 3 for potentials (Fig. 4B) more negative than -65 mV comparable to that observed in Ref. [9]. The control or wild-type recovery time constant for -85 mV was 15.6 ms while the mutant time constant was 46.8 ms. The filled circles in Fig. 3 represent measurements of the RP, the VP and p(UP) for a cable of mutant channels. For each value of G_{Na} , slowed recovery from inactivation amplified the RP, the VP and p(UP) when compared with the wild type cells (filled squares).

Other mutations of the Na channel accelerate inactivation and have also been associated with arrhythmogenic processes [9,19–21]. Accelerated inactivation will reduce the peak Na current during phase I of the action potential, equivalent to a reducing G_{Na} , thus slowing conduction. We tested this hypothesis by doubling the rate of fast inactivation, β_f , which reduced the inactivation time constant at 0 mV from 180 to 90 μ s. With $G_{Na}=24.25$ mS/cm², the conduction velocity was reduced from 64.65 to 50.96 cm/s, and the refractory period was extended from 456.2 to 468.4 ms while the VP was prolonged from 1.9 to 5.1 ms.

Plotting VP against the reciprocal s1 conduction velocity for both normal and mutant (slowed recovery) channels

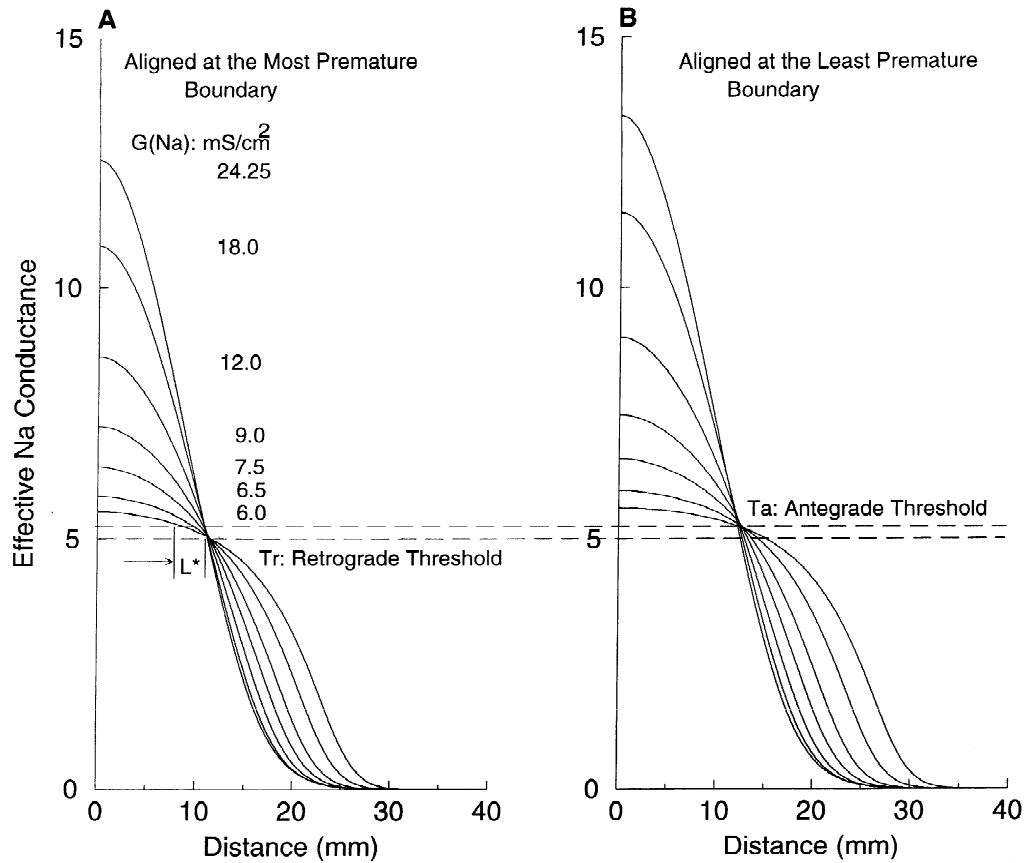


Fig. 2. Spatial profiles of restoration conductance or effective Na channel conductance, $g_{Na}(x) = G_{Na} h(x) j(x)$, at s1-s2 delays associated with the transition from block to stable retrograde propagation (A) and the transition to stable antegrade propagation (B). Alignment of the conductance profiles associated with the boundaries of the VP revealed common intersections, equivalent to thresholds for stable retrograde and stable antegrade propagation. Due to the restoration gradient of Na channel conductance, a wave propagating in the retrograde direction is able to recruit more recovered Na channels per space constant than a wave propagating in the less recovered antegrade direction. Ignoring the recruiting mechanism, the VP represents the time for the retrograde threshold to propagate across the stimulus field: $VP = L/v$ where L is the length of the field and v is the s1 wave velocity. However, the asymmetry of Na channel conductance at the s2 site during the VP means that the recruited channels per space constant will be less for antegrade extension of the front than for retrograde extension of the front. When the s1-s2 delay aligns the retrograde threshold with the right edge of the s2 electrode, the antegrade front collapses due an insufficient I_{Na} . The s1-s2 delay must be extended in order move the retrograde threshold point beyond the right edge of the electrode, thus compensating for the smaller antegrade I_{Na} . This additional time permits the s1 wave to travel an additional distance, L^* . Shown in panel A is the distance, L^* , required for the $G_{Na} = 6 \text{ mS/cm}^2$ profile to travel in order to recruit enough Na channels to sustain stable antegrade propagation.

(Fig. 5A) revealed a non-linear relationship. Earlier models of the VP [3,13] were based on negligible s2 front development time and a common threshold for stable retrograde and antegrade propagation. These assumptions led to a linear relationship between VP and $1/\text{velocity}$:

$VP = L/v$. However Fig. 1C,G demonstrated that the antegrade front development process was sensitive to G_{Na} and Fig. 2 revealed different thresholds for stable retrograde and antegrade propagation. We incorporated these observations into the W-R model by estimating the

Table 1
Vulnerable period measurements: variations in G_{Na}

G_{Na} (mS/cm ²)	RP (ms)	VP (ms)	s1 Velocity (cm/s)	$dg_{Na}(x_r)/dx$ mS/cm ² per cm	$dg_{Na}(x_a)/dx$ mS/cm ² per cm
6.0	500.7	11.2	31.059	-0.10112	-0.071936
6.5	488.6	8.2	33.434	-0.16000	-0.124928
7.5	477.9	5.7	37.235	-0.25523	-0.22656
9.0	471.0	4.2	41.688	-0.38169	-0.358912
12.0	464.8	3.1	48.382	-0.56781	-0.561664
18.0	459.3	2.4	57.710	-0.77082	-0.781056
24.25	456.2	1.9	64.646	-0.88269	-0.900352

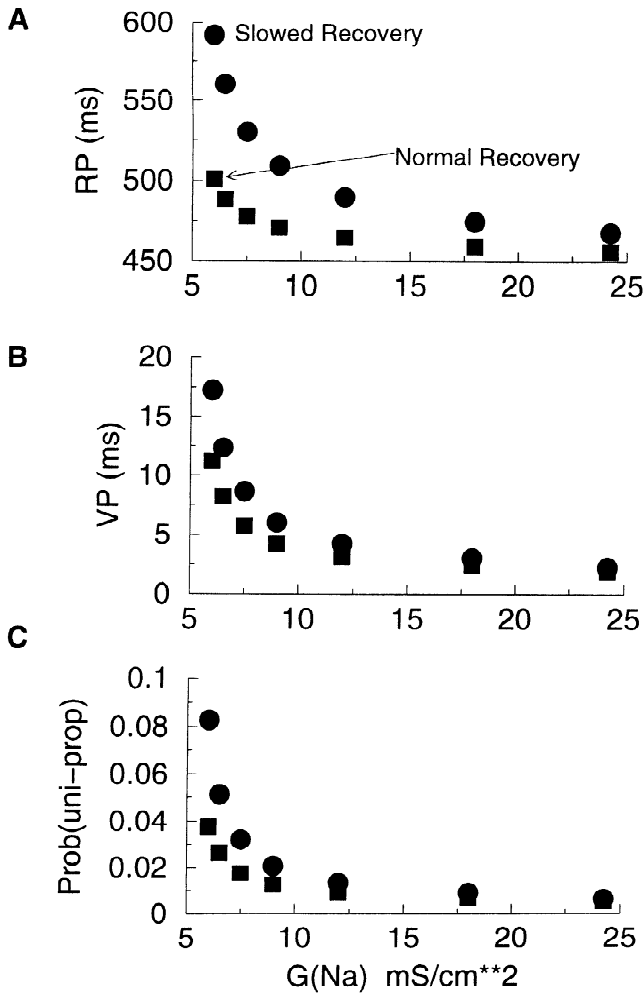


Fig. 3. The maximum macroscopic Na conductance, G_{Na} , altered the refractory period (RP, panel A), the vulnerable period (VP, panel B) and the probability of unidirectional propagation (Prob, panel C). The filled squares represent normal recovery from inactivation while the filled circles represent retarded recovery from inactivation associated with a mutation that reduced the recovery rate 3-fold. Reducing G_{Na} increased the RP, VP and Prob in both cases with the increases being more pronounced with slowed recovery than with normal recovery.

additional distance the s1 wave must travel in order for the availability at the right boundary of the s2 stimulus field to exceed the threshold for stable antegrade propagation. This distance is $L^* = \delta/dg_{Na}(x_r)/dx$, where $\delta = T_r - T_a$, the difference between the two availability thresholds and is depicted in Fig. 2A.

Incorporating the gradient term, the VP is described by:

$$VP = \frac{L + \delta/dg_{Na}(x_r)/dx}{v} = \frac{L + L^*}{v} \quad (2)$$

where L is the length of the suprathreshold stimulus field, L^* is the virtual extension of the stimulus field and v is the s1 propagation velocity. Least squares fitting of the data to Eq. (2) resulted in excellent fits (solid lines, $r=0.99$) for both control and slowed recovery from inactivation (Fig. 5A).

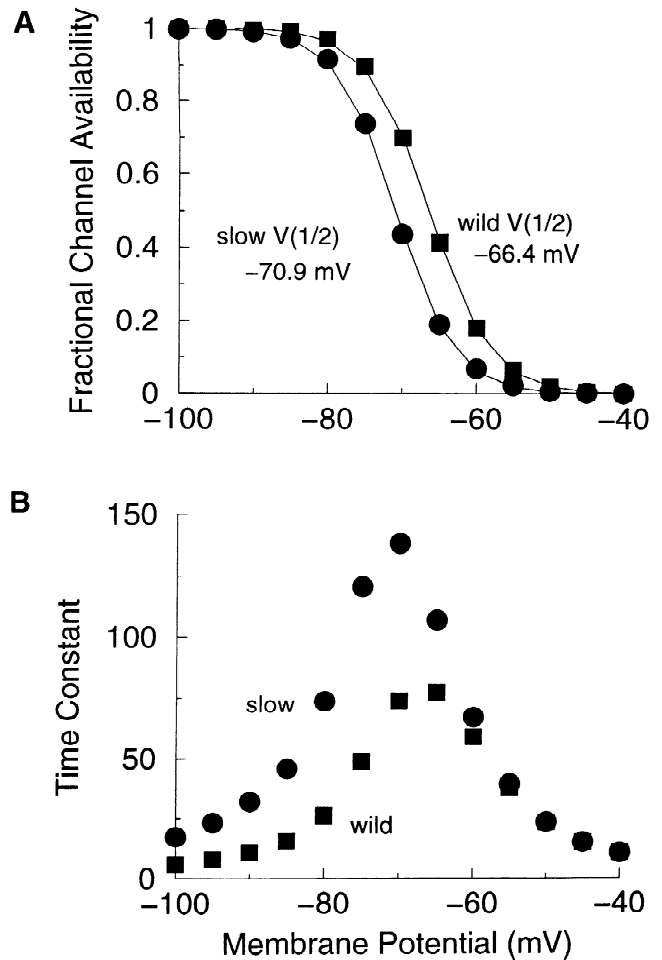


Fig. 4. The membrane potential dependence of the fractional channel availability (panel A) and the time constant of recovery from inactivation (panel B). Reducing the inactivation recovery rate by 3 shifted the availability curve 4.5 mV in the hyperpolarizing direction similar to observed values [10] and increased the time constant of inactivation recovery by 3 at potentials less than -65 mV. At -85 mV the recovery time constant slowed from 15.5 to 46.5 ms.

The Na conductance restoration gradient is directly linked to the inactivation recovery rate as follows:

$$\frac{\partial G_{Na}hj}{\partial x} = \frac{\partial G_{Na}hj}{\partial t} \frac{1}{v} \quad (3)$$

Thus, if we know the rate of recovery from channel inactivation, we can approximate the gradient and estimate the VP with only channel parameters. In cardiac cells, inactivation recovery is dominated by the time constant for recovery from ‘slow’ inactivation. Thus, Eq. (2) can be written in terms of the slow inactivation recovery time constant, τ_j , the retrograde threshold fraction of non-inactivated channels, $(hj)_{crit}$, and the difference in the retrograde and antegrade conductance threshold, δ as:

$$VP = \frac{L}{v} + \frac{\delta\tau_j}{G_{Na}(hj)_{crit}} \quad (4)$$

We tested this relationship by varying the transition rate

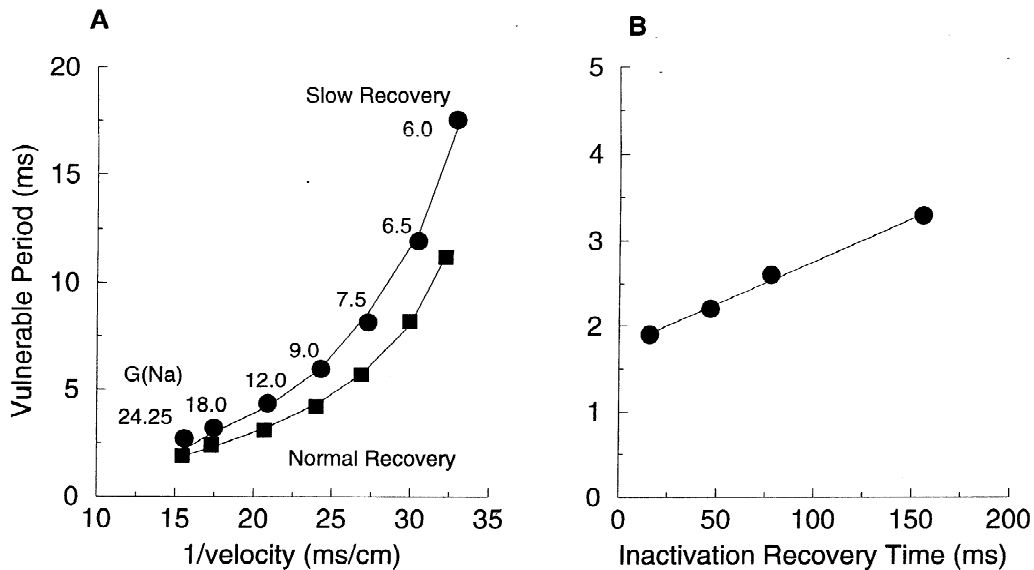


Fig. 5. The vulnerable period as a function of $1/s1$ velocity (panel A) and the time constant of recovery from inactivation (panel B). (A) The VP in the absence of availability gradient effects represents the time required for the retrograde threshold to cross the s2 stimulus field: $VP = L/v$ where L is the length of the s2 field and v is the velocity of the s1 wave. Panel A shows the VP for values of G_{Na} ranging from 24.25 to 6.0 mS/cm^2 (near the threshold of propagation) and reveals that as the conduction velocity was reduced, the VP increased at a rate exceeding that predicted by the linear, gradient free model. Least squares fitting of a model incorporating the gradient effect (Eq. (2)) resulted in excellent agreement between observed and predicted values (solid line). Slowing the recovery rate from channel inactivation reduced the availability gradient within the VP at the s2 site and increased the VP for each value of Na conductance. The solid line is the least squares fit of the mutant data. (B) The restoration gradient within the VP at the s2 site is proportional to the time constant of recovery from inactivation (Eq. (4)). Shown here is the predicted linear relationship between VP and the recovery time constant ($r > 0.99$).

from inactive to non-inactivated channels, α_j , over a range of 10, determining the VP and plotting the results (Fig. 5B). The s1 velocity was insensitive to the changes in the inactivation recovery rate, thus the first term in Eq. (4) was constant while the second term varied with τ_j . The data were well fit by a straight line, $r = 0.99$ (solid line) confirming this simplification.

4. Discussion

An absolute prerequisite for reentry is the formation of a premature impulse within a vulnerable region, where impulse propagation succeeds in some directions and fails in other directions. However, many factors contribute to propagation success and failure, including the dispersion of refractoriness [22], the ability to excite a region larger than the liminal length [23,24] and the presence of anisotropic coupling between cells [25]. In a structurally complex multi-dimensional preparation, the length of the excitation wave relative to the size of the excitable tissue mass places an additional constraint on whether reentry can be sustained.

Vulnerability, a generic property of any excitable medium, requires only an excitation threshold, a refractory process and diffusive coupling [3] and can be readily demonstrated in chemical media [26]. Cardiac cells share these properties and, to develop an understanding of modulators of excitability, refractoriness and coupling on

the VP, it is first necessary to establish baseline responses in a minimally complex medium. Here we used a one-dimensional cable of identical cardiac cells as a basis for exploring how the vulnerable period is impacted by changes in Na channel function. With this foundation, follow-on studies can focus on whether tissue and cellular complexities such as spatial variations in cellular refractoriness and anisotropic cellular connectivity amplify or attenuate the underlying proarrhythmic mechanism. Additional complexities (pumps, currents, complex connectivity, etc.) can only extinguish vulnerability by extinguishing either excitability, refractoriness or coupling, features that are essential for a functional heart.

The duration of the VP is critically dependent on the dynamics of recruiting the requisite density of Na channels necessary to sustain propagation in either the retrograde or antegrade direction. The boundaries of the VP depend on the interaction between the density of recruited channels and the thresholds for retrograde/antegrade propagation. Following an s1 wave, retrograde recruiting is more efficient than antegrade recruiting because the density of recovered channels per space constant is greater in the retrograde direction. This asymmetry results in a conductance threshold for stable antegrade propagation that is greater than that for stable retrograde propagation. During the restoration process, re-excitation either: (i) fails because the density of recruited channels is less than that required for either stable antegrade or retrograde propagation; (ii) is incomplete because the density of retrograde

recruited channels exceeds the retrograde threshold but the density of antegrade recruited channels falls below the antegrade threshold; or (iii) succeeds because the density of recruited channels in both directions exceeds the antegrade threshold. Incomplete excitation is proarrhythmic and represents unidirectional propagation in a cable and a wave break (leading to spiral waves) in two- and three-dimensional tissue. Thus the duration of the VP depends on both the time course of conductance restoration and the velocity of the s1 wave as shown in Eqs. (2) and (4). That a flattening of the Na conductance restoration gradient linked with arrhythmogenic processes is supported by a number of reports.

Proarrhythmia is associated with infarcted and ischemic myocardium, yet the underlying mechanisms are uncertain. In studies of myocytes dispersed from the epicardial border zone in recently infarcted canine hearts, Pu and Boyden [10] reported reductions in the density of Na channels, accelerated inactivation and slowed recovery from inactivation. A missense mutation (Thr1620Met) in SCN5A, identified in patients with Brugada syndrome, was found to both speed the decay of the inward Na current as well as prolong the recovery from inactivation [8,19]. Accelerated inactivation was identified with another missense mutation (Glu567Leu) in SCN5A, which was linked with sudden infant death and Brugada syndrome [20]. Similarly Vatta and colleagues [21] identified Na channel mutants in cases of sudden unexplained nocturnal death syndrome (SUNDS) and identified mutations that accelerated the rate of Na channel inactivation. The substitution (D1790G) in SCN5A resulted in a hyperpolarizing shift in the steady-state inactivation curve [2]. Our studies demonstrate a common denominator, flattening the conductance gradient at the site of re-excitation, that is shared by these mutants. Slowed recovery from inactivation directly flattens the restoration gradient. Reduced expression of Na channels, hyperpolarizing shifts in steady-state inactivation and accelerated inactivation all reduce the peak Na current and indirectly flatten the restoration gradient.

We utilized these observations to refine the W–R model of the vulnerable period [3]. Shown in Fig. 6 is a one-dimensional cable with a conditioning wave propagating from left to right. Shown also is the conductance wave. During the last moments of repolarization, Na channels begin to recover from inactivation and the effective Na conductance, g_{Na} , increases. As the cells continue their recovery from inactivation, the effective conductance crosses the threshold for stable retrograde conduction, T_r . The s1–s2 delay determines the position of T_r relative to the s2 site. Small s1–s2 delays produce collapsing fronts, as these test stimuli fall within the refractory period. As the s1–s2 delay is extended, the transition point, T_r , crosses the s2 stimulus field and initiates a retrograde wave while the antegrade directed front collapses, a result of inadequate density of recruited non-inactivated channels in the antegrade direction. The W–R model of the vulnerable period is based on the time required for the retrograde

threshold to pass over the extent of the s2 stimulus field: L/v where L is the length of the electrode and v is the velocity of the conditioning wave. However, when the s1–s2 delay is such that T_r coincides with the right boundary of the s2 field, the antegrade conductivity is below the threshold for stable retrograde propagation. Consequently the antegrade front collapses. Additional s1–s2 delay is necessary in order to overcome the effects of antegrade propagation into a below-threshold region. The additional delay is determined by the time required for the restored conductance at the right boundary of the s2 site to exceed the antegrade threshold, T_a . This distance for $G_{Na}=6 \text{ mS/cm}^2$ is indicated by L^* in Fig. 2, is labeled virtual extension in Fig. 6 and is computed as $L^* = (T_r - T_a)/d(g_{Na}(x_r)/dx)$.

The implications of the restoration of Na conductance (and its gradient) in determining the vulnerable period are far reaching. The disparity in conductance thresholds for stable antegrade and retrograde propagation follows directly from the asymmetry (gradient) in Na conductance recruiting densities in the retrograde and antegrade directions. The slower the restoration process, the flatter the restoration gradient and the greater the time required to exceed the antegrade threshold. Similarly reductions in G_{Na} (or apparent G_{Na}) flatten the restoration gradient. This provides a mechanistic basis for understanding why acceleration of inactivation and reductions in Na channel density, inactivation recovery rates and use-dependent drug unblocking rates all affect the VP in a similar manner: all flatten the restoration gradient thus increasing L^* and prolonging the VP.

The rate of recovery from inactivation of both normal and mutant sodium channels is steeply voltage dependent (Fig. 4B), so that changes in the shape of action potential repolarization (phase 3) can significantly alter the Na conductance restoration process. Specifically, action potentials with a steep phase 3 repolarization have been demonstrated to be less proarrhythmic than those with a more triangular repolarization morphology [27]. Thus drugs that alter late repolarizing currents may also alter the VP through modulation of the membrane potential driven Na conductance restoration process. Similarly, defibrillation creates complex patterns of potential distribution with regions of depolarized potentials and other regions of hyperpolarized potentials. Recent studies [28] have demonstrated the influence of polarity of the defibrillation pulse on success or failure of defibrillation, an effect that may well be linked to altering gradients of Na conductance in vulnerable regions.

Recognition of the role of the Na conductance restoration gradient led to a new model for the VP that incorporated the Na channel recruiting process. This model suggests a new strategy for assessing the proarrhythmic potential associated with a mutant channel. When the s1 velocity is constant, the VP was directly proportional to the time constant for restoring channel conductance. With Eq. (4) it is possible to evaluate the proarrhythmic potential of

Model of the Vulnerable Period

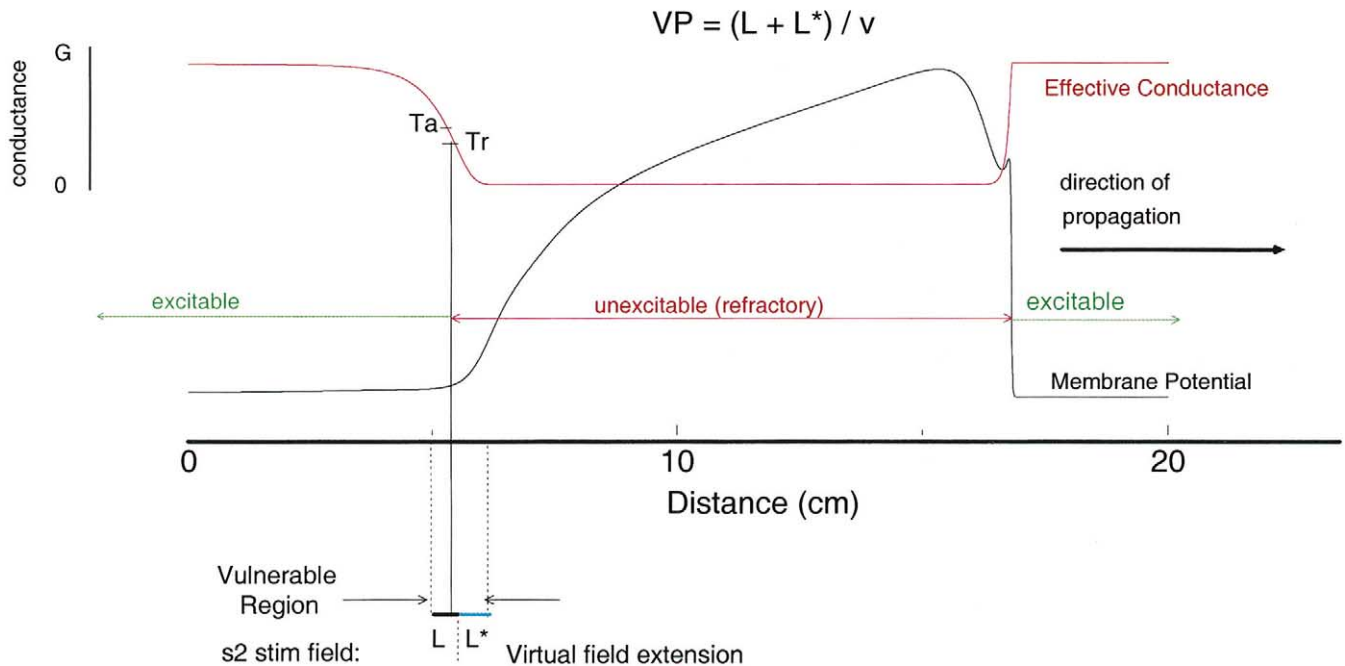


Fig. 6. A model of the cardiac vulnerable period. Shown is a snapshot of an action potential (AP) as it propagates with velocity, v , from left to right along a one-dimensional cable. At time of the snapshot, the refractory-excitability boundary (T_r) falls within the s2 stimulation field (thick black line). Shown also is the conductance wave (g_{Na} , red) and the vulnerable region produced by the interaction between the s2 stimulus field and the refractory-excitability boundary that trails the AP. Within the conductance recovery wave are two critical conductances: T_r , the minimum conductance required to establish stable retrograde propagation and T_a , the minimum conductance required to establish stable antegrade propagation. Following s2 stimulation, antegrade and retrograde fronts evolve in a manner determined by the conductance recovery profile. Stable propagation results if the front is able to recruit an adequate density of Na channels in the direction of propagation. The absolute magnitude of Na conductance and the spatial gradient of Na conductance determine the wave front recruiting potential. Because the antegrade front must propagate into less recovered medium, the threshold for stable antegrade propagation is greater than the threshold for stable retrograde propagation. Unidirectional propagation results when T_r falls within the suprathreshold region of the stimulus field, L , and its virtual extension, L^* . Timing a stimulus such that T_r falls within the suprathreshold region triggers unidirectional propagation characterized by an antegrade front that propagates decrementally and eventually collapses, a result of inadequate Na channel recruiting capacity and a retrograde front that evolves to a stably propagating retrograde wave, a result of propagating into a more recovered region. Bidirectional propagation from s2 stimulation is possible only after T_r passes beyond L^* (cyan), where T_a is aligned with the right boundary of the s2 stimulus field. Thus the VP represents the time required for T_r to traverse both the physical s2 stimulation field (black), L , and the virtual extension (cyan), $L^* = (T_a - T_r) / dg_{Na} / dx$. The transit time of T_r across $L + L^*$ defines the VP as $(L + L^*) / v$.

mutant structures directly from channel transition rates and channel conductance. These relationships should prove useful in future investigations.

References

- [1] Mines GR. On circulating excitations in heart muscle and their possible relation to tachycardia and fibrillation. *Trans R Soc Can* 1914;8:43–52.
- [2] Wiggers CF, Wegria R. Ventricular fibrillation due to single localized induction and condenser shocks applied during the vulnerable phase of ventricular systole. *Am J Physiol* 1940;128:500–503.
- [3] Wiener N, Rosenbluth A. The mathematical formulation of the problem of conduction of impulses in a network of connected excitable elements, specifically in cardiac muscle. *Arch Inst Cardiol Mex* 1946;16:205–265.
- [4] Allesie MA, Bonke FIM, Schopman FJG. Circus movement in rabbit atrial muscle as a mechanism of tachycardia. *Circ Res* 1973;33:54–62.
- [5] VanCapelle FJL, Durrer D. Computer simulation of arrhythmias in a network of coupled excitable elements. *Circ Res* 1980;47:454–466.
- [6] Joyner RW. Mechanisms of unidirectional block in cardiac tissues. *Biophys J* 1981;35:113–125.
- [7] Quan W, Rudy Y. Unidirectional block and reentry of cardiac excitation: a model study. *Circ Res* 1990;66:367–382.
- [8] An RH, Wang XL, Kerem B et al. Novel LQT-3 mutation affects Na⁺ channel activity through interactions between α - and β_1 -subunits. *Circ Res* 1998;83:141–146.
- [9] Dumaine R, Towbin JA, Brugada P et al. Ionic mechanisms responsible for the electrocardiographic phenotype of the Brugada syndrome are temperature dependent. *Circ Res* 1999;85:803–809.
- [10] Pu J, Boyden PA. Alterations of Na⁺ currents in myocytes from epicardial border zone of the infarcted heart: a possible ionic mechanism for reduced excitability and postrepolarization refractoriness. *Circ Res* 1997;81:110–119.
- [11] The Cardiac Arrhythmia Suppression Trial (CAST) Investigators. Preliminary report: effect of encainide and flecainide on mortality in a randomized trial of arrhythmia suppression after myocardial infarction. *N Engl J Med* 1989;432:406–412.
- [12] Starmer CF, Lastra AA, Nesterenko VV, Grant AO. A proarrhythmic response to sodium channel blockade: theoretical model and numerical experiments. *Circulation* 1991;84:1364–1377.

- [13] Starmer CF, Viktashev VN, Romashko DN, Stepanov MR, Makarova ON, Krinsky VI. Vulnerability in an excitable medium: analytical and numerical studies of initiating unidirectional propagation. *Biophys J* 1993;65:1775–1787.
- [14] Starmer CF, Lancaster AR, Lastra AA, Grant AO. Cardiac instability amplified by use-dependent Na channel blockade. *Am J Physiol* 1992;262:H1305–H1310.
- [15] Nesterenko VV, Lastra AA, Rosenshtraukh LV, Starmer CF. A proarrhythmic response to sodium channel blockade: modulation of the vulnerable period in guinea pig ventricular myocardium. *J Cardiovasc Pharmacol* 1992;19:810–820.
- [16] Starmer CF, Grant AO, Colatsky TJ. What happens when cardiac Na channel function is compromised? 2: Numerical studies of the vulnerable period in tissue altered by drugs (accepted for publication).
- [17] Beeler GW, Reuter H. Reconstruction of the action potential of ventricular myocardial fibers. *J Physiol* 1977;268:177–210.
- [18] Ebijara L, Johnson EA. Fast sodium current in cardiac muscle: a quantitative description. *Biophys J* 1980;779–790.
- [19] Bezzina CR, Rook MB, Wilde AAM. Cardiac sodium channel and inherited arrhythmia syndromes. *Cardiovasc Res* 2001;49:257–271.
- [20] Wan X, Chen S, Sadeghpour A, Wang Q, Kirsch GE. Accelerated inactivation in a mutant Na⁺ channel associated with idiopathic ventricular fibrillation. *Am J Physiol* 2001;280:H354–H360.
- [21] Vatta M, Dumaine R, Varghese G et al. Genetic and biophysical basis of sudden unexplained nocturnal death syndrome (SUNDS), a disease allelic to Brugada syndrome. *Hum Mol Genet* 2002;11:337–345.
- [22] Alessi R, Nusynowitz M, Abildskov JA, Moe GK. Non-uniform distribution of vagal effects on the atrial refractory period. *Am J Physiol* 1958;194:406–410.
- [23] Rushton WAH. Initiation of the propagated disturbance. *Proc R Soc B* 1937;124:210–243.
- [24] Fozzard HA, Schoenberg M. Strength-duration curves in cardiac Purkinje fibres: effects of liminal length and charge distribution. *J Physiol* 1972;226:593–618.
- [25] Spach MS, Dolber PC, Heidlage JF. Interaction of inhomogeneities of repolarization with anisotropic propagation in dog atria: a mechanism for both preventing and initiating reentry. *Circ Res* 1989;65:1612–1631.
- [26] Gomez-Gesteira M, Fernandez-Garcia G, Munuzuri A et al. Vulnerability in an excitable Belousov-Zhabotinsky medium: from 1D to 2D. *Physica D* 1994;76:359–368.
- [27] Hondeghem LM, Carlsson L, Duker G. Instability and triangulation of the action potential predict serious proarrhythmia, but action potential duration prolongation is antiarrhythmic. *Circulation* 2001;103:2004–2013.
- [28] Yamanouchi Y, Cheng Y, Tchou PJ, Efimov IR. The mechanism of the vulnerable window: the role of virtual electrodes and shock polarity. *Can J Physiol Pharmacol* 2001;79:25–33.